New particle formation in anthropogenic plumes advecting from Asia observed during TRACE-P

R. J. Weber,[1] S. Lee,[1] G. Chen,[2] B. Wang,[1] V. Kapustin,[3] K. Moore,[3] A. D. Clarke,[3] L. Mauldin,[4] E. Kosciuch,[4] C. Cantrell,[4] F. Eisele,[1,4] D. C. Thornton,[5] A. R. Bandy,[5] G. W. Sachse,[2] and H. E. Fuelberg[6]

Received 31 October 2002; revised 6 March 2003; accepted 19 March 2003; published 11 November 2003.

[1] The characteristics and sources of what are believed to be newly formed 3 to 4 nm particles in anthropogenic plumes advecting from Asian are reported. Airborne measurements were made from March to April 2001 as part of the NASA TRACE-P experiment at latitudes ranging from North of the Philippines to Northern Japan (20 to 45°N). In the more polluted plumes, high concentrations of 3 to 4 nm diameter particles (>100cm^{-3}) were observed both within and along the upper outer edges of plumes that were identified by enhanced carbon monoxide and fine particulate sulfate concentrations. The results from two research flights are investigated in detail. Three to four-nm particle concentrations are generally correlated with gas phase sulfuric acid and found in regions of low surface areas relative to the immediate surroundings or where there are steep transitions to lower surface areas. Sulfuric acid and surface area concentrations in the most polluted plume reached 6×10^7 cm^{-3} and 750 μm^2 cm^{-3}, respectively, in regions of particle formation. In contrast to these anthropogenic plumes, few 3 to 4 nm particles were observed in the clean background and few were detected within a volcanic plume where the studies highest H_2SO_4 concentrations (>10^8 cm^{-3}) were recorded. Enhanced SO_2 concentrations in the range of approximately 2 to 7 ppb, in conjunction with other unidentified, possibly coemitted species, appear to be the driving factor for nucleation. *INDEX TERMS:* 0305 Atmospheric Composition and Structure: Aerosols and particles (0345, 4801); 0322 Atmospheric Composition and Structure: Constituent sources and sinks; 0345 Atmospheric Composition and Structure: Pollution—urban and regional (0305); 4801 Oceanography: Biological and Chemical: Aerosols (0305); *KEYWORDS:* atmospheric aerosol, homogeneous nucleation, sulfuric acid, nanoparticles, gas-to-particle conversion

Citation: Weber, R. J., et al., New particle formation in anthropogenic plumes advecting from Asia observed during TRACE-P, *J. Geophys. Res.*, *108*(D21), 8814, doi:10.1029/2002JD003112, 2003.

1. Introduction

[2] Atmospheric aerosols play a role in the global climate through their influence on the Earth's radiation balance. The scattering of solar and terrestrial radiation by aerosols depends on the ambient particle number distribution and particle composition, which are influenced by the rate and prevalence of new particle formation. On more regional scales the source of nanometer-sized particles is of scientific interest due to their possible adverse health effects. Several epidemiological studies [*Donaldson et al.*, 1998; *Ferin et al.*, 1990] have found that ultrafine particles less than 50 nm are correlated to adverse pulmonary diseases, and large increases in the concentration of ultrafine particles due to homogeneous nucleation have been observed in urban areas [*Woo et al.*, 2001].

[3] Owing to their possible climate and health effects, many investigations have been conducted into the mechanism of new particle formation, but the details are still unknown because of the complexity of the process and current measurement limitations. There are inadequate theories and a lack of thermodynamic data for multicomponent nucleation. The primary measurement limitation is that nucleation produces new particles of approximately 1 nm in diameter; however, current measurement techniques can only detect particles down to roughly 3 nm in diameter, which is significantly larger than the newly formed particles. Thus evidence for nucleation is only detected some time following the event, once the newly formed particles have grown to detectable sizes.

[1]School of Earth and Atmospheric Sciences, Georgia Institute of Technology, Atlanta, Georgia, USA.
[2]NASA Langley Research Center, Hampton, Virginia, USA.
[3]Department of Oceanography, University of Hawaii at Manoa, Honolulu, Hawaii, USA.
[4]National Center for Atmospheric Research, Boulder, Colorado, USA.
[5]Department of Chemistry, Drexel University, Philadelphia, Pennsylvania, USA.
[6]Department of Meteorology, Florida State University, Tallahassee, Florida, USA.

0148-0227/03/2002JD003112$09.00

[4] Previous work suggests that H_2SO_4 often is a nucleation precursor, since nucleation events, indicated by unusually high concentrations of 3–4 nm or concentrations of 3–10 nm diameter particles, is correlated with H_2SO_4 concentrations. In the past, binary H_2SO_4-H_2O homogeneous nucleation has been considered as the most likely nucleation mechanism. However, previous studies, in which H_2SO_4 and nm-sized particles were measured, find that observed particle formation rates cannot be explained by classical binary nucleation theory [*Birmili et al.*, 2000; *Birmili and Wiedensohler*, 2000; *Weber et al.*, 1995, 1996, 1997, 1998a, 1999].

[5] Ternary nucleation [*Coffman and Hegg*, 1995; *Korhonen et al.*, 1999] has been proposed as a mechanism that may explain the observations. Experiments show that adding NH_3 to the binary H_2SO_4-H_2O system can increase the rate of new particle formation [*Ball et al.*, 1999]. Some workers have found new particle formation where NH_3 is expected to play a role [*Birmili et al.*, 2000; *Weber et al.*, 1998a]. An ion-mediated nucleation mechanism is also a possible route for particle formation [*Yu and Turco*, 2001].

[6] Although many studies have focused on nucleation in remote regions, evidence for nucleation under polluted conditions has also been observed. Increased particle concentrations have been detected at the edges of power plant and smelter plumes [*Brock et al.*, 2003; *Wilson*, 1978; *Williams et al.*, 1981]. In some cases, the newly formed particles are often found at the edges of relatively fresh plumes (<2 hours old) [*Brock et al.*, 2003] where photochemical models predict highest hydroxyl radical (OH) concentrations and enhanced production of H_2SO_4 by oxidation of SO_2. New particle formation has been observed in urban settings, such as Atlanta, Georgia [*McMurry et al.*, 2000]. In this case, evidence for nucleation was based on events when the sub 10-nm size distribution tailed off to higher concentrations as sizes approached the detection limit of 3 nm. *McMurry et al.* [2000] suggest that nucleation in Atlanta may be explained by a collision-controlled process involving H_2SO_4.

[7] One objective of the National Atmospheric and Space Administration (NASA) Transport and Chemical Evolution over Pacific (TRACE-P) mission was to investigate the mechanisms and conditions of particle production associated with Asian plumes emanating from the densely populate regions of China, Korea, and Japan. *Jacob et al.* [2003] provides an overview of the TRACE-P experiment. This mission provided an opportunity to sample plumes with varying characteristics, including biomass, volcanic, and urban pollution plumes. We find that high concentrations of 3 to 4nm particles are only associated with the pollution plumes. This paper describes the conditions where evidence for recent nucleation was observed from two research flights and briefly investigates the nucleation mechanism by contrasting the various observations.

2. Instrumentation

[8] The intensive measurement component of TRACE-P ran from February through April 2001. The aim of this multiinvestigator experiment was to characterize air masses advected from Asia to gain insights into the physical and chemical processing of gases and aerosol particles in Asian plumes. Two NASA aircraft were involved, a DC-8 and P3-B. Each aircraft made nine flights near the Asian continental regions to characterize Asian outflow. This paper focuses on the P-3B measurements of sulfur dioxide (SO_2), sulfuric acid (H_2SO_4), and aerosols.

[9] Sulfur dioxide (SO_2) was measured by an atmospheric pressure ionization mass spectrometer (APIMS) [*Thornton et al.*, 2002]. Sulfuric acid and the hydroxyl radical (OH) were measured by chemical ionization mass spectrometry (CIMS) [*Eisele et al.*, 1993, 1994, 1997]. A number of instruments were deployed for measurements of aerosol number concentration. A modified ultrafine condensation particle counter (TSI 3025, St. Paul, Minn.) equipped with pulse height analysis (PHA-UCPC) measured ultrafine condensation particle concentrations at 1 Hz. Referred to as ultrafine condensation nuclei, this includes all particles larger than ~3 nm in diameter. Pulse height analysis also allows measurements of concentrations of particles between 3 and 10 nm diameter integrated over 30s. The technique provides information on nanoparticle spectra. We have developed approaches to invert measured pulse height distributions to obtain 3 to 10 nm size distributions [*Weber et al.*, 1998b]. However, a simpler approach is used in which only the smallest pulses are counted to determine particle concentrations in a narrow diameter range at the instrument's lower detection limit (e.g., ~3 to 4 nm). Although only an estimate of the concentration, this technique is highly sensitive and useful when searching for regions of new particle formation since one can focus on only the most recently formed nanoparticles.

[10] A limitation with this technique is that by converting to white-light optics necessary for pulse height analysis [*Marti et al.*, 1996], the optical detection region is not as highly focused as in the commercial TSI 3025 UCPC, which uses a laser diode. This results in a greater time for individual particles to transit the scattering region of the detector, which increases the probability that more than one particle will be in the scattering region at one time. This so-called coincidence will result in an undercounting of particles when concentrations are high. A dilution system was employed to extend the upper concentration range of the instrument. However, at UCN concentrations higher than approximately 10,000 cm^{-3}, coincidence becomes significant and the UCN measurements are more uncertain (on the order of ±50%). Further under measurement is possible, especially when nanoparticles are present, due to losses in the roughly 5-m long sample line running from the inlet to the PHA-UCPC. The UCN and 3 to 4-nm particle concentrations reported in this paper are converted to standard temperature and pressure (20°C and 1 atmosphere).

[11] Ambient aerosol size distributions of fine and coarse particles were measured with a variety of instruments. Our interest is in the interaction of the gases (e.g., H_2SO_4) and newly formed particles with the preexisting aerosol, which requires a measurement of the aerosol number distribution. Measurements of the dry (heated to 40°C) distribution of particles between 0.15 and 19 μm was made in the aircraft cabin via a shrouded isokinetic inlet with an Optical Particle Counter (OPC, PMS LAS-X, Boulder, Colo.). Because the inlet temperature was cycled to investigate changes in the distribution to particle volatility, size distributions were integrated over 1 min but often measured only once every

Table 1. List of Measurements, Techniques, Institutions, and Principle Investigators (PI) for the Data Used in This Analysis[a]

Measurement	Technique	Institution	PI
SO_2	APIMS	Drexel	R. Bandy/D. Thornton
H_2SO_4	CIMS	NCAR	F. Eisele
CO	DACOM	NASA Langley	G. Sachse
Ultrafine CN	PHA-UCPC	Georgia Tech	R. Weber
3–4 nm particles	PHA-UCPC	Georgia Tech	R. Weber
Aerosol Surface Area	Optical particle counter, 0.15 to 19 μm diameter	U. of Hawaii	A. Clarke
Fine Particle Ionic Compounds	PILS/IC	Georgia Tech	R. Weber

[a]APIMS: atmospheric pressure ionization mass spectrometer; CIMS: chemical ionization mass spectrometer; DACOM: differential absorption CO measurement, fast response tunable diode laser sensors measured carbon monoxide spectroscopically; PHA-UCPC: Pulse height analysis-ultrafine condensation particle counter; PILS/IC: particle into liquid sampler coupled to dual channel ion chromatograph.

3 min. Ambient wet particle size distributions are estimated by assuming accumulation mode particles (diameters less than 0.6 μm diameter) absorb water as a generic marine aerosol [*Swietlicki et al.*, 2000], and coarse mode particles behave as dust and do not absorb water. The measured surface areas are uncertain for a number of reasons: (1) Inlet and sampling losses of particles with diameters larger than approximately 3 μm. (2) Losses of semivolatile material, other than water, on heating the particles to 40°C. (3) Uncertainties associated with converting the dry distribution to ambient size distributions by calculating the aerosol particle uptake of water.

[12] A wing-mounted Forward Scattering Spectrometer Probe 300 (FSSP; 0.3 ∼ 20 μm diameter) provided particle liquid water content data, which was used to identify spurious UCN data due to sampling artifacts associated with droplet shatter on the aerosol sampling inlet [*Weber et al.*, 1998c]. Evidence of shatter has been removed from the data set for this analysis.

[13] The bulk ionic composition of fine particles was measured continuously and in near real-time with a Particle Into Liquid Sampler, PILS [*Orsini et al.*, 2003; *Weber et al.*, 2001b]. The anions (chloride, nitrate, and sulfate) and cations (sodium, ammonium, potassium, magnesium, and calcium) were measured at a rate of every 4 min. Table 1 summarizes the main gaseous and particle components used in this analysis along with the measurement technique, institution, and principle investigator.

3. Theory

[14] In the following discussion, a number of factors are calculated to aid in the analysis. This includes the sulfuric relative acidity, the loss of H_2SO_4, and newly formed 1.5-nm-diameter particles by preexisting particle scavenging, and the production rate of H_2SO_4 and its predicted steady state concentration.

3.1. Sulfuric Relative Acidity

[15] Classical nucleation theory predicts that nucleation rates depend on the degree of vapor saturation [e.g., *Wilemski*, 1984]. A measure of H_2SO_4 vapor saturation is the sulfuric relative acidity (RA). RA is calculated from the measured H_2SO_4 concentration (this includes all monoacid hydrates), divided by the saturation concentration of pure acid over a flat surface, given as the partial pressure in atmospheres (p) by *Ayers et al.* [1980] as:

$$p = \exp(-10156/T + 16.259) \quad (1)$$

where T is the absolute temperature.

3.2. Scavenging of H_2SO_4 and 1.5 nm Diameter Particle

[16] The rates of H_2SO_4 and 1.5-nm particle loss by absorption onto the preexisting aerosol particles is calculated using the method of *Fuchs and Sutugin* [1970] as we have done in other studies [*Eisele and Tanner*, 1993; *Jefferson et al.*, 1998; *Weber et al.*, 2001a; *Weber et al.*, 1997]. For the calculation of H_2SO_4 scavenging, an accommodation coefficient of 0.72 is assumed [*Jefferson et al.*, 1997] and the hydrated H_2SO_4 molecule diffusivity of 0.08 cm2 s^{-1} [*Roedel*, 1979] is used. The effect of ambient temperature and RH on monomer mass is estimated from bulk properties [*Gmitro and Vermeulen*, 1963] and used to calculate the monomer average thermal speed.

[17] Scavenging losses of newly formed particles are estimated by calculating the loss of a 1.5 nm diameter particle, as a surrogate for particles between 1 and 3 nm in diameter, using the same method as that for H_2SO_4. In this case, we assume an accommodation coefficient of 1, and the 1.5 nm-particle thermal speed is calculated as a function of temperature and a constant relative humidity of 50%, and a calculated diffusivity. In both calculations, the inverse of the Fuchs-Sutugin first order loss rate constant (k', units 1/s) is the characteristic (*e-folding*) scavenging time.

3.3. H_2SO_4 Production Rates and Calculated Steady State Concentrations

[18] The rate at which H_2SO_4 vapor is produced is calculated by:

$$R = k[OH][SO_2] \quad (2)$$

where the rate constant, k depends on ambient temperature and pressure and ranges from 7 to 9 × 10^{-13} cm^{-3} s^{-1} [*DeMore et al.*, 1992]. Since the H_2SO_4 scavenging rates (k') are high in these plumes, H_2SO_4 is likely in a steady state balance between production and loss. This is a good approximation since typical H_2SO_4 lifetimes are in the range of less than one minute to four minutes (see Table 2). The calculated steady state acid concentration is then:

$$[H_2SO_4]_c = R/k'. \quad (3)$$

In the following analysis, consistency between SO_2, H_2SO_4 and the preexisting ambient aerosol distribution is assessed by comparing measured H_2SO_4 concentrations to $[H_2SO_4]_c$.

4. Observations

[19] TRACE-P was conducted from March to mid-April from two bases of operation. Flights were first made from

Table 2. Measured and Calculated Conditions of Nucleation and No Nucleation Regions for Two Case Study Flights (F19 and F14) and Volcanic Plume (F17) During TRACE-P[a]

	Mean	Median	Max	Min	Standard Deviation
(A) Nucleation Above Plume - Case Study One - Sea of Japan - Flight 19, N = 16					
Altitude, km	1.57	1.41	2.11	1.39	0.27
Temperature, K	275	275.5	276	273	0.9
RH, %	33	32.5	44	18	7.7
CO, ppbv	203	208	257	153	29
SO_2, pptv	1,679	1,752	2,884	588	652
OH, $cm^{-3}(\times 10^6)$	4.60	4.39	6.85	3.05	1.12
H_2SO_4, $cm^{-3}(\times 10^7)$	2.40	2.07	3.59	1.71	0.68
Relative Acidity$(\times 10^{-4})$	8.20	7.75	12.50	5.79	0.19
3–4 nm particle, cm^{-3}	175	139	431	82	95
UCN, cm^{-3}	10,472	10,313	13,149	7,325	1,781
Surface Area, $\mu m^2 cm^{-3}$	26	23	42	15	9.8
SO_4^{2-}, pptv	196	96	645	47	229
NH_4^+, pptv	677	402	1983	143	687
NH_4^+/SO_4^{2-} molar ratio	4.5	4.35	6	3.5	1
k′ 1.5 nm, $s^{-1}(\times 10^{-3})$	1.2	0.82	0.24	4.0	1.1
k′. H_2SO_4, $s^{-1}(\times 10^{-3})$	4.1	3.0	0.76	13	3.6
(B) No Nucleation Within Plume - Case Study One - Sea of Japan - Flight 19, N = 13					
Altitude, km	0.42	0.3	0.93	0.11	0.26
Temperature, K	282	282	285	277	2.6
RH, %	68	77	79	47	15
CO, ppbv	323	326	342	261	21
SO_2, pptv	2,288	2,365	3,218	1,047	520
OH, $cm^{-3}(\times 10^6)$	8.02	7.88	13.7	5.31	2.30
H_2SO_4, $cm^{-3}(\times 10^7)$	1.97	1.72	3.10	1.38	0.57
Relative Acidity$(\times 10^{-4})$	3.20	2.77	5.81	1.39	1.67
3–4 nm particle, cm^{-3}	1	1	1.6	0.5	0.23
UCN, cm^{-3}	5,080	4,984	6,665	4,022	691
Surface Area, $\mu m^2 cm^{-3}$	171	182	217	111	34
SO_4^{2-}, pptv	2,618	2,739	3,133	1,565	525
NH_4^+, pptv	6,006	6,407	7,141	2,767	1,343
NH_4^+/SO_4^{2-} molar ratio	2.7	2.7	2.8	2.6	0.08
k′ 1.5 nm, $s^{-1}(\times 10^{-3})$	3.0	3.1	1.4	4.8	0.79
k′ H_2SO_4, $s^{-1}(\times 10^{-3})$	9.2	9.4	5.1	14.7	2.5
(C) Nucleation - Case Study Two - Yellow Sea - Flight 14, N = 13					
Altitude, km	0.21	0.12	0.66	0.12	0.18
Temperature, K	284	284	286	282	1.2
RH, %	51	52.5	75	32	12.8
CO, ppbv	675	703	806	503	94
SO_2, pptv	7,882	7,629	10,217	5,613	1,471
OH, $cm^{-3}(\times 10^6)$	10.8	10.7	15.0	7.41	1.74
H_2SO_4, $cm^{-3}(\times 10^7)$	5.95	6.28	8.83	2.78	2.22
Relative Acidity$(\times 10^{-4})$	6.72	6.47	11.3	3.68	2.43
3–4 nm particle, cm^{-3}	198	190	330	113	60
UCN, cm^{-3}	11,896	12,285	14,440	8,211	2,108
Surface Area, $\mu m^2 cm^{-3}$	744	735	1830	29	606
SO_4^{2-}, pptv	5,265	5,636	6,136	3,920	898
NH_4^+, pptv	17,435	19,262	20,133	3,354	19,262
NH_4^+/SO_4^{2-} molar ratio	3.75	3.73	3.8	3.7	0.05
k′ 1.5 nm, $s^{-1}(\times 10^{-3})$	3.87	4.12	2.5	9.4	3.2
k′ H_2SO_4, $s^{-1}(\times 10^{-3})$	14	15	0.93	32	11
(D) No Nucleation - Case Study Two - Yellow Sea - Flight 14, N = 3					
Altitude, km	0.12	0.12	0.12	0.12	0
Temperature, K	282	282	282	282	0
RH, %	85	86	86	84	1.2
CO, ppbv	661	654	692	636	29
SO_2, pptv	3,188	3,190	3,605	2,768	419
OH, $cm^{-3}(\times 10^6)$	10.5	10.5	11.8	9.28	1.26
H_2SO_4, $cm^{-3}(\times 10^7)$	1.56	1.53	1.77	1.37	2.01
Relative Acidity$(\times 10^{-4})$	2.27	2.23	2.58	2.0	0.29
3–4 nm particle, cm^{-3}	1	1	1	1	0
UCN, cm^{-3}	5,821	5,813	6,025	5,626	200
Surface Area, $\mu m^2 cm^{-3}$	1618	1553	1423	1879	235
SO_4^{2-}, pptv	4,040	4,040	4,040	4,040	0
NH_4^+, pptv	15,448	15,448	15,448	15,448	0
NH_4^+/SO_4^{2-} molar ratio	4.4	4.4	4.4	4.4	0
k′ 1.5 nm, $s^{-1}(\times 10^{-3})$	8.2	7.7	7.2	9.6	1.2
k′ H_2SO_4, $s^{-1}(\times 10^{-3})$	25	23	21	32	5.7

Table 2. (continued)

	Mean	Median	Max	Min	Standard Deviation
(E) Volcanic Plume[b] *- Flight 17, N = 30*					
Altitude, km	0.34	0.34	1.15	0.16	0.19
Temperature, K	286	286	289	279	2.06
RH, %	58	58	65	53	3.5
CO, ppbv	217	214	234	195	5.3
SO_2, pptv	8,087	8,157	17,458	4,179	3,204
OH, $cm^{-3}(\times 10^6)$	3.7	3.6	5.3	2.2	0.57
H_2SO_4, $cm^{-3}(\times 10^7)$	7.9	7.3	16.3	5.3	2.5
Relative Acidity$(\times 10^{-4})$	7.0	5.9	15.8	2.2	2.9
3–4 nm particle, cm^{-3}	2.8	2.3	6.5	0.98	1.4
UCN, cm^{-3}	5,796	5,033	9,652	2,628	2,323
SO_4^{2-}, pptv	2,391	2,151	4,135	1,213	969
NH_4^+, pptv	2,222	1,888	3,284	1,278	665
NH_4^+/SO_4^{2-} molar ratio	0.98	0.95	1.45	0.53	0.2

[a]N is number of data points, except for surface area and scavenging time, which have fewer points and k′ is the rate constant for loss of 1.5 nm particles or H_2SO_4 onto the preexisting aerosol determined from the method of *Fuchs and Sutugin* [1970].

[b]The scavenging rate constants for H_2SO_4 and 1.5-nm particles are not included in the table for the volcanic plume since surface area size distributions are not available.

Hong Kong, China from 5 to 16 March 2001. The aircraft was then based out of Yokota Air Force Base near Tokyo, Japan between 17 March and 3 April 2001. The geographical region investigated is shown in Figure 1. A variety of plumes were sampled during the study and identified by the gaseous and fine particle chemical components. High CO, SO_2, and fine particle sulfate (SO_4^{2-}) concentrations identify anthropogenic plumes. CO and SO_2 indicate combustion sources. SO_4^{2-} is from gas-to-particle conversion of anthropogenic SO_2 and provides a measure of the aerosol loading, assuming that the biogenic SO_2 sources in this region are small in comparison to the anthropogenic emissions. There is also a volcanic SO_2 source from Miyaka-Jima, in southern Japan, which is identified by high SO_2 concentrations and a lack of CO. This was a major source of SO_2 during the TRACE-P experiment [*Tang et al.*, 2003].

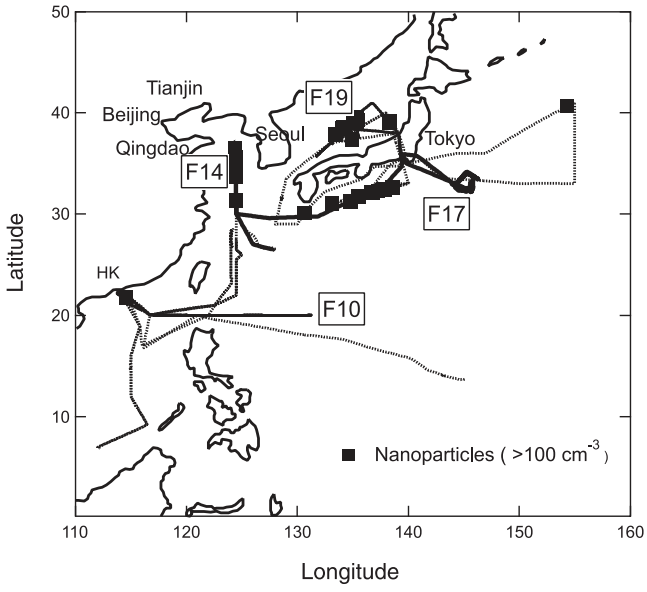

Figure 1. Flight paths near the Asian continental regions during TRACE-P and regions of high 3 to 4-nm particle concentration (>100 cm^{-3}).

Fine particle potassium and CO, along with other species, identified biomass burning emissions. The role of biomass burning on fine particle composition is discussed by *Ma et al.* [2003].

[20] Several flights with plumes of unique characteristics and the regions with high 3–4 nm particle concentration are also highlighted in Figure 1. Frequent encounters with well-defined plumes were made near the Asian continental areas during the TRACE-P experiment. For example, in flight 10 a relatively pure biomass plume was identified; a volcanic plume on flight 17 and encounters with large anthropogenic plumes during flights 14 and 19 are also identified in Figure 1.

[21] Three to four-nm particles were not observed in the biomass plume (flight 10) which contained low SO_2 concentrations measured at ~200 pptv and correspondingly low H_2SO_4 concentrations at less than 2×10^6 cm^{-3}. Apparently, no organic species nucleated to form new particles in the biomass plume in the region sampled. The volcanic plume (flight 17) had high SO_2 concentrations, but contained only low 3 to 4 nm particle concentrations (<10 cm^{-3}, see Table 2e) suggesting that there was little particle production in this plume when our measurements were made. In contrast, high 3 to 4-nm particle concentrations (>100 cm^{-3}) were often observed in anthropogenic plumes. Of these, the most extensive regions of new particle formation observed during TRACE-P were recorded on flights 14 and 19. 3 to 4-nm particle production associated with these plumes is investigated in detail in the following sections.

4.1. Case Study 1: Sea of Japan, Flight 19

[22] Figure 2 shows the flight path over the Sea of Japan and identifies the pollution plumes. Florida State University's Kinematic Trajectory Model, using the three wind components derived from the European Center for Medium-Range Weather Forecasts (ECMWF), calculated 5-day back-trajectories. For more detail, see *Fuelberg et al.* [2000] and *Maloney et al.* [2001]. The back-trajectory analysis in Figure 2 illustrates that the air masses sampled had passed over the highly populated and industrial regions

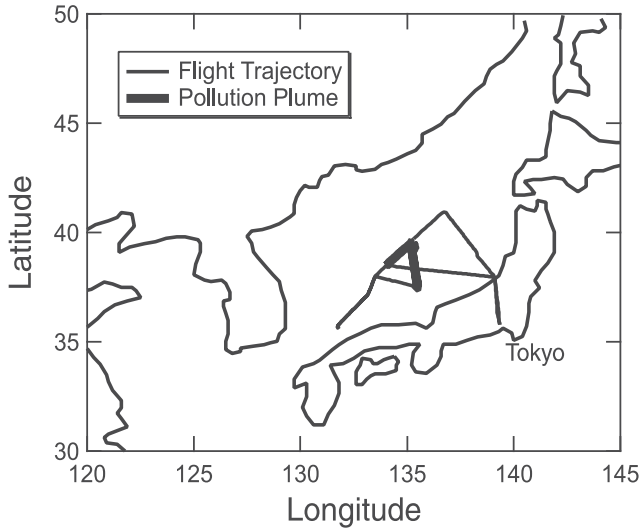

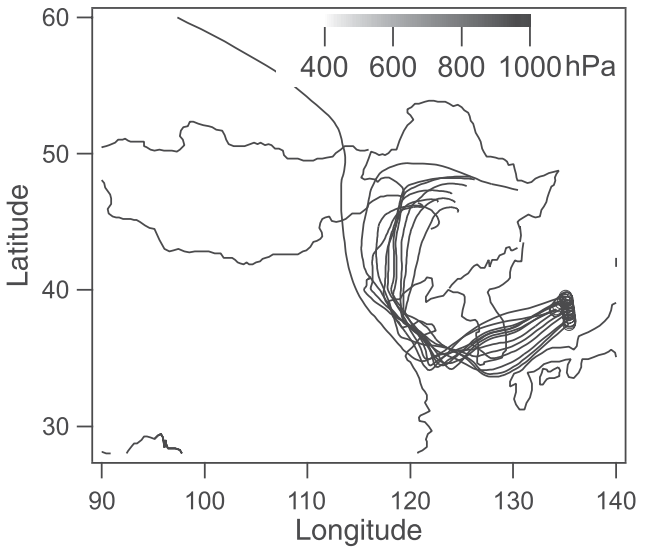

Figure 2. Flight 19 path and 5-day back trajectories for case 1, Sea of Japan. The region of plume interception is identified.

of western China and may have been impacted by the cities of Beijing, Tianjin, or Qingdao. The plumes then traveled across the Yellow Sea and South Korea below 1 km altitude prior to entering the Sea of Japan. These air masses likely acquired pollutants from urban centers in both China and Korea. Here we focus on the flight conducted in the vicinity of 38°N latitude and 135°E longitude between roughly 1100 ∼ 1330 local Sun time.

[23] The time series of various measurements near and within the plume are shown in Figure 3. The altitude shows a number of soundings and horizontal legs during this period, the longest leg was below 1 km above sea level (asl). Based on CO and SO_4^{2-} concentrations in Figure 3b, a large anthropogenic plume was intercepted and constrained to altitudes below approximately 1.5 km asl. Although the two surface level measurements where the plume is detected are actually made in different regions in the Sea of Japan (see Figure 2), the back-trajectory analysis indicates that both plumes likely had a similar origin, suggesting it may be a single large plume. Figure 3c shows that the H_2SO_4 and SO_2 concentrations also increased with the CO and SO_4^{2-} concentrations and that H_2SO_4 and SO_2 are fairly well correlated.

[24] UCN (all particles larger than 3 nm) in Figure 3d are also enhanced in the plumes and generally follow the CO concentration defining the plume boundaries. Three to four-nm particles are near zero at the higher altitudes above the plume and also within the plume during the lowest altitude leg near the ocean surface. However, high concentrations are detected in distinct regions; these regions are highlighted in Figure 3 by the shaded vertical bands. Comparison of these 3 to 4-nm particle regions with altitude shows that over this wide geographical region where the aircraft sampled in and out of the plume, there is a well defined altitude range between roughly 1 and 2.7 km asl

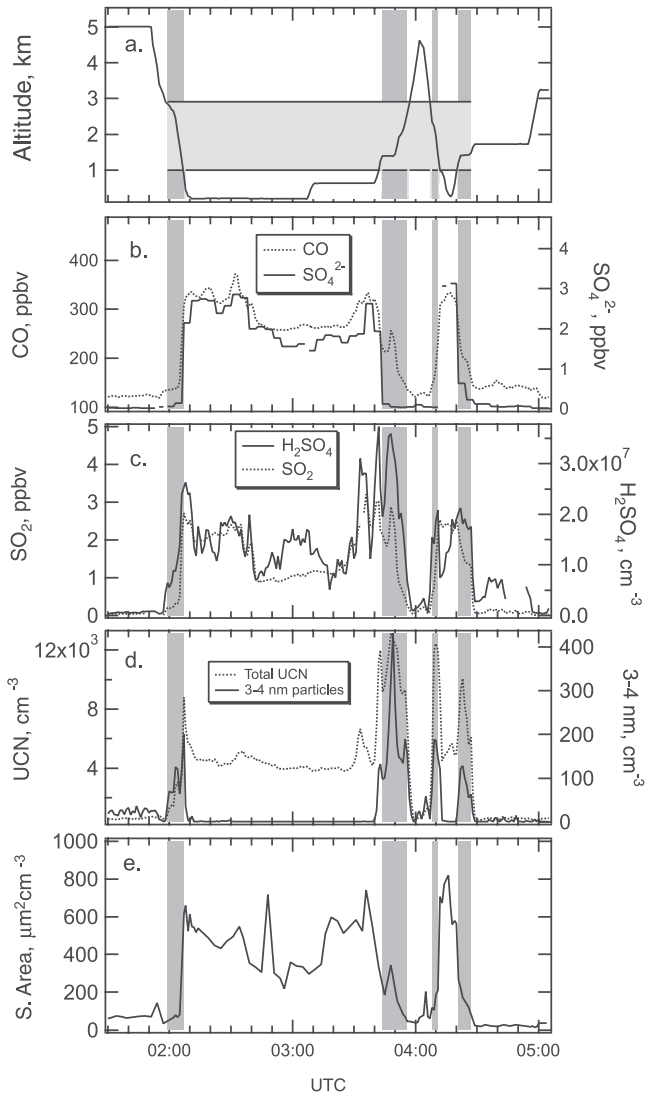

Figure 3. Time series plots for case 1 (Sea of Japan, flight 19) with (a) altitude, (b) CO and SO_4^{2-}, (c) SO_2 and H_2SO_4, (d) UCN and 3 to 4-nm particles, and (e) aerosol surface area. Shading identifies regions of 3 to 4-nm particle production.

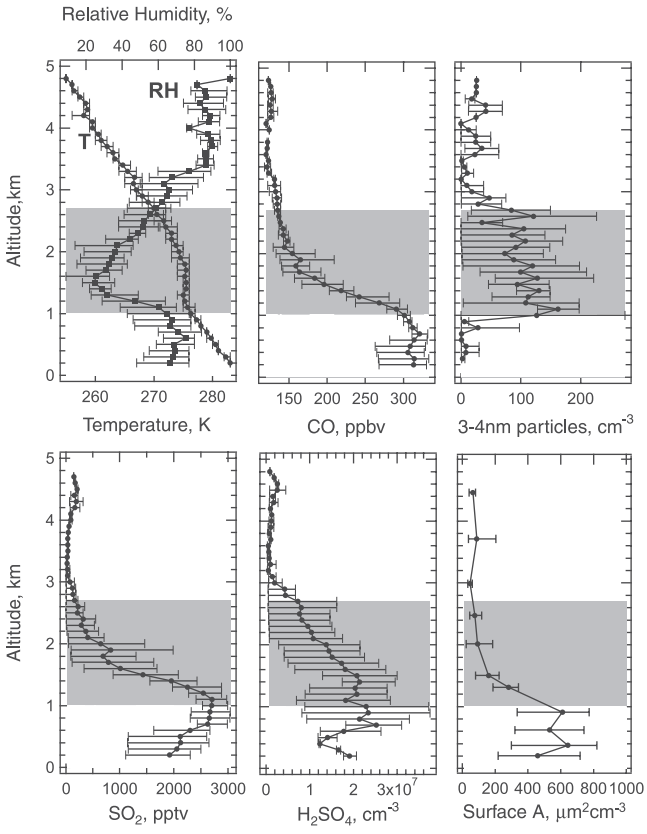

Figure 4. Vertical profiles for the four soundings of case 1, Sea of Japan, flight 19 shown in Figure 3. The mean is plotted and max/min are shown as error bars.

where 3 to 4-nm particles are always detected. The cross-hatched box in Figure 3a identifies the altitude of this region.

[25] High 3 to 4-nm and UCN particles (shaded areas in Figure 3) appear to be associated with the high H_2SO_4 concentrations and suggests that H_2SO_4 may have participated in new particle production in these regions. However, note that there are regions within the plume near the ocean surface where concentrations of H_2SO_4 are similar to the 3 to 4-nm particle regions but where 3 to 4-nm particle concentrations are very low. These regions have much higher aerosol surface area concentrations, whereas the 3 to 4-nm particle regions are found where surface areas are lowest. On average, the characteristic lifetime of a 1.5 nm particle ($1/k'$) within the plumes is about 6 min, compared with 14 min in the 3 to 4-nm regions. These and various other measurements in the 3–4 nm particle regions and within the plume that lacked nucleation are summarized in Tables 2a and 2b, respectively.

[26] The unique 3–4 nm particle regions associated with this plume are investigated in more detail by plotting the vertical profiles. Means from the four separate soundings, and the "error bar," indicating maximum and minimum measurements, are shown in Figure 4. The shaded region in each graph in Figure 4, spanning 1.0 to 2.7 km asl, is the region of enhanced 3 to 4-nm particle concentrations. The temperature profile shows a weak inversion at about 1.0 km asl. The band of 3 to 4-nm particles is found mainly above the inversion in a dryer layer, as seen by the relative humidity profile. CO concentrations, which identify the location of the plume, begin to decrease above 1 km asl as the plume is diluted into the cleaner air above. This is the region where 3 to 4-nm particle concentrations start to increase with altitude.

[27] SO_2 levels tend to follow the CO, with the exception that they begin to decrease at a slightly higher altitude of 1.3 km asl, overlapping the lower altitude region of 3 to 4-nm particles. H_2SO_4 has a similar vertical trend; it generally follows both CO and SO_2 but on average does not begin to decrease until higher altitudes. Notice that highest H_2SO_4 concentrations are found right at the inversion, on the upper edge of the plume. Aerosol surface areas are highest in the plume, then drop above the plume, similar to CO.

[28] The fine particle ionic composition of the plume is shown in Figure 5. In this case, concentrations are given as mass at 20°C and 1 atmosphere pressure. The measured cations and anions are nearly balanced. The molar equivalence ratio of cations minus anions to the sum of all ions is less than 1%. Furthermore, sulfate and nitrate are nearly balanced by ammonium, suggesting that the main ionic components of the fine aerosol particles are ammonium sulfate and ammonium nitrate salts.

4.2. Case Study 2: Yellow Sea Plume, Flight 14

[29] In contrast with the Sea of Japan plume, a plume comprised of some of the highest CO, SO_2 (with the exception of the volcanic plume-flight 17) and fine particle sulfate and nitrate of the entire TRACE-P mission was intercepted at the surface in the Yellow Sea at 35°N latitude and 124.5°E longitude (see Figure 6). Back trajectories indicate that the surface level air masses were arriving directly from the west, a path similar to the plume intercepted in the Sea of Japan, detailed in case study 1 above, which may have picked up pollution from the large cities such as Tianjin and Qingdao, China. In this case the plume was likely intercepted closer to its main source. Ratios of $SO_4^{2-}/(SO_4^{2-} + SO_2)$, which can provide a measure of plume age, are smaller in this plume than those of Flight 14; this suggests that the plume is fresher (Ft 14 ratio is 0.42 and Ft 19, 0.51).

[30] This plume was intercepted on the lowest altitude leg, below 1 km asl, at roughly 1200 ~ 1300 local Sun time. Time series plots, similar to those for the Sea of Japan

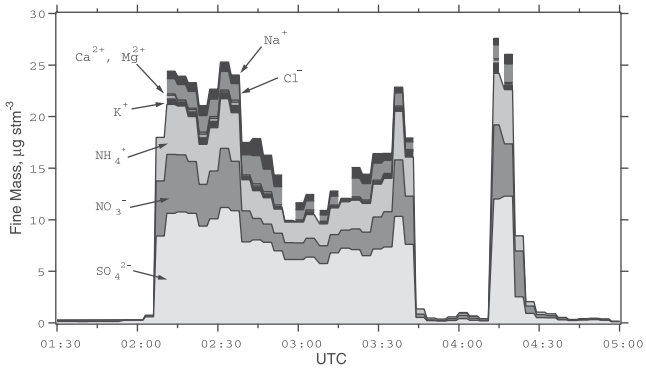

Figure 5. Fine particle (Dp < 1.3 μm) ionic mass in case study 1, Sea of Japan plume. Mass concentrations are at 20°C and 1 atmosphere. An ion balance suggests most sulfate and nitrate is balanced by ammonium.

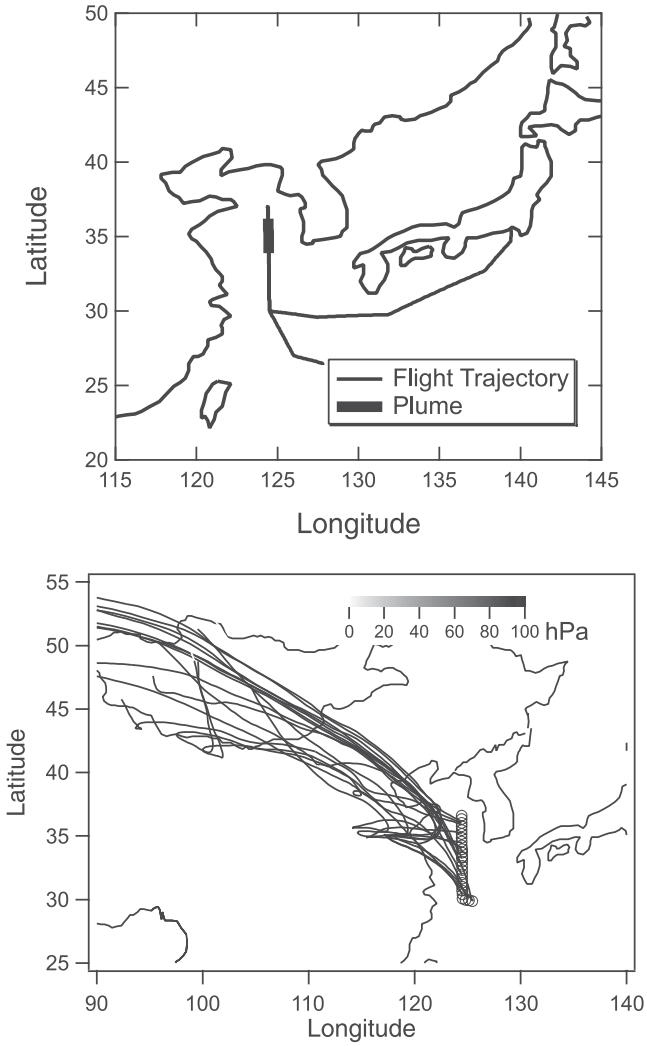

Figure 6. Flight 14 path and 5-day back trajectories for case 2, Yellow Sea plume. The region of plume interception is identified.

plume of Case 1, are shown in Figure 7. CO and SO_4^{2-} concentrations identify the plume, which in this case are about double those of the Sea of Japan plume in Figure 3. SO_2 and H_2SO_4 track almost precisely. (This is likely a result of the very short H_2SO_4 lifetime due to rapid scavenging and the high acid production rates, which is discussed in the following section). Both SO_2 and H_2SO_4 have peak concentrations that are the highest for the complete TRACE-P mission, except those in the volcanic plumes (Miyake-Jima, Japan) of flight 17. Note that H_2SO_4 data is only available during the first half of the plume measurement.

[31] Concentrations of UCN and 3 to 4-nm particles, shown in Figure 7d, also roughly track the CO, SO_4^{2-}, SO_2, and H_2SO_4. The shaded area in Figure 7a identifies the altitude ranges where 3to 4-nm particles are detected. This range can vary in altitude from the surface up to 1.8 km asl, and up to 3.4 km asl. In this plume, 3 to 4-nm particles are observed both in regions slightly above the plume and completely throughout the plume, with the exception of the plume center where RH is greater than 85%. Again, nanoparticle concentrations tend to be highest in regions of higher SO_2 and H_2SO_4.

[32] Aerosol surface area concentrations increase toward the center of the plume where the relative humidity is over 85%. In this central region, CO and SO_4^{2-} concentrations were slightly lower, and SO_2 and H_2SO_4 were significantly reduced. No 3 to 4-nm particles were found in this region. The data from the two3 to 4-nm bands are summarized in Table 2c, and the region of no 3–4 nm particles is summarized in Table 2d.

[33] Vertical profiles are plotted in Figure 8. In this case, two soundings were made and data from both are plotted. Temperature profiles show that the boundary layer was very shallow, with an inversion at 30 m asl. Based on CO concentrations, the plume extended considerably above the inversion to about 1.8 to 2 km asl. SO_2 and H_2SO_4 concentrations are highly correlated. However, unlike the Sea of Japan plume, the 3 to 4-nm particles in this case are not as well correlated with H_2SO_4. The figure shows that 3 to 4-nm particles are found throughout the plume and into the dilution region above it.

[34] The plume's fine particle ionic composition is shown in Figure 9. Note the much higher concentrations compared

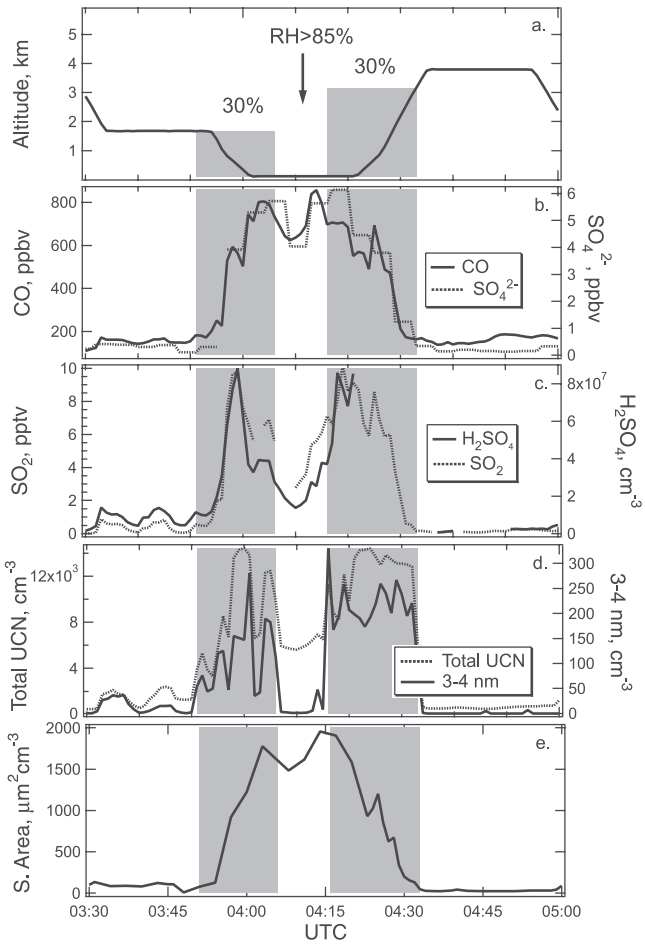

Figure 7. Time series plots for case 2, Yellow Sea, flight 14 with (a) altitude, (b) CO and SO_4^{2-}, (c) SO_2 and H_2SO_4, (d) UCN and 3 to 4-nm particles, and (e) aerosol surface area. Shading identifies regions of 3 to 4-nm particle production.

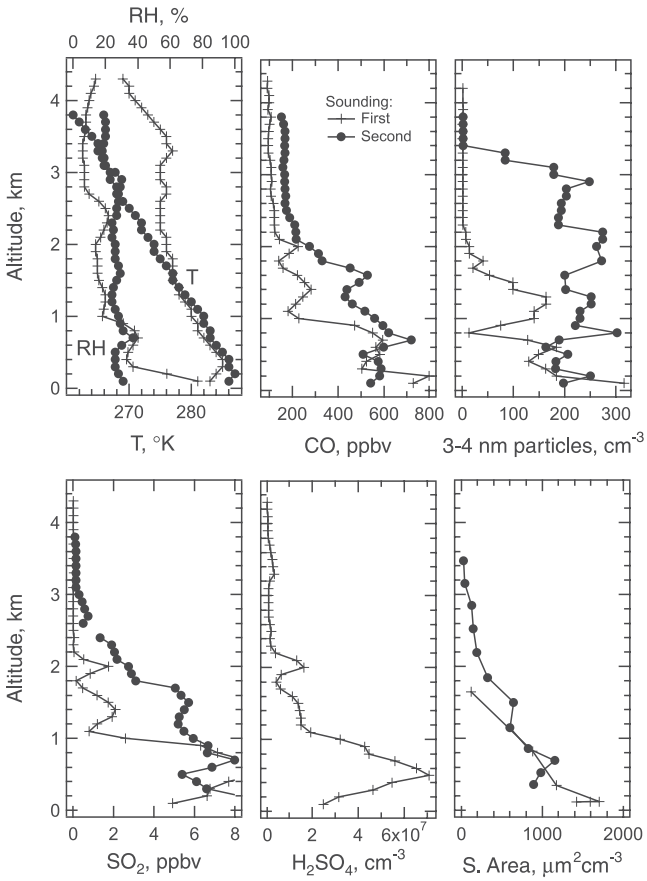

Figure 8. Vertical profiles for the two soundings of the Yellow Sea plume of flight 14, case 2 in Figure 7. (a) Relative humidity and temperature, (b) CO, (c) 3 to 4-nm particles, (d) SO_2, (e) H_2SO_4, and (f) aerosol surface area.

with case 1 in Figure 6. This plume is unusual in that nitrate concentrations exceed sulfate. An ion balance suggest that most of the sulfate and nitrate is associated with ammonium (e.g., $(NH_4)_2SO_4$ and NH_4NO_3). Another interesting feature of this plume is the potassium concentrations (K^+), which are the highest recorded during this mission and are thought to be associated with biomass burning emissions [*Ma et al.*, 2003].

[35] Not all plumes investigated in this study show evidence of nanoparticle production. During flight 19 in the Sea of Japan, two other anthropogenic plumes were intercepted on horizontal legs at less than 1 km asl. In this case, SO_2 concentrations are much lower, (near ~0.2 ppbv), as are both H_2SO_4, with an average concentration of 3×10^6 cm^{-3}, and 3 to 4-nm particle concentrations, which averaged less than 1 cm^{-3}. These case studies and the apparent lack of particle production in plumes of low H_2SO_4 concentrations point to the role of H_2SO_4 in particle production and indirectly to the importance of SO_2 concentrations.

5. Discussion

[36] Concentrations of newly formed nanoparticles depend on the homogeneous nucleation rate and the rate at which they are lost and dispersed. Because the timescales for nanoparticle scavenging near and within these polluted plumes are very small, on the order of 5 to 15 min (1/k′, Table 2), particle loss by dry deposition, dispersion, and dilution are in comparison of minor importance. It follows then that highest 3 to 4-nm concentrations would be expected in regions of highest nucleation rates (i.e., precursor concentrations, such as H_2SO_4) and lowest scavenging rates (i.e., lowest 3 to 4-nm mass transfer rate constants, k′, or roughly aerosol surface area concentrations). For a given plume, this is generally consistent with the observations. In each plume the 3 to 4-nm particles tend to be associated with high acid concentrations and found where surface areas are low or rapidly decreasing with respect to the immediate surroundings. This is most clearly seen in the case 1 Sea of Japan plume in Figure 3 where 3 to 4-nm particles are found in the regions of highest H_2SO_4 concentrations where the area is low but not in the plume at similar acid level where the surface area is high.

[37] Another consequence of the high scavenging rates of H_2SO_4 and 3 to 4-nm particles is that their concentrations will respond rapidly to changes in ambient conditions. Thus the conditions where 3 to 4-nm particles are observed are likely very close to those in which homogeneous nucleation occurred. It is also noted that the high scavenging rates of newly formed particles imply that particle growth rates must also be too high to compensate or else few newly formed particles would be detected.

[38] Contrasting the nucleation regions of the two pollution plumes also provides some insights into conditions under which particle production can occur. There are significant differences in the regions of homogeneous nucleation for the two plumes discussed above. For example, despite higher H_2SO_4 mass transfer rates to the preexisting particles (H_2SO_4 k′) in the Yellow Sea plume, H_2SO_4 concentrations were on average three times higher in the nanoparticle regions (see Figures 3 and 7 and Table 2). This implies that the production rate of H_2SO_4 must have been considerably higher in this plume to offset its loss by particle scavenging and to maintain the higher acid concentrations. The average H_2SO_4 production rates in the more polluted Yellow Sea plume (Flight 14, case 2) are 1×10^6 cm^{-3} s^{-1}, about an order of magnitude higher than those in the Sea of Japan plume (Flight 19, case 1) which average at 2×10^5 cm^{-3} s^{-1}. A comparison shows that the high acid production rate is due to higher concentrations of both SO_2 and OH. However, larger SO_2 appears to be the

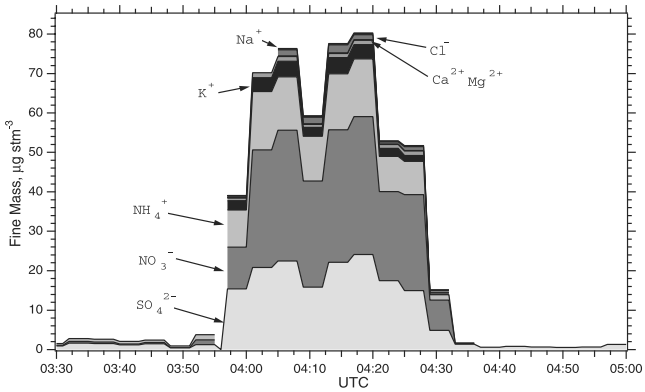

Figure 9. Fine particle ionic composition for Yellow Sea plume, case study 2, Flight 14.

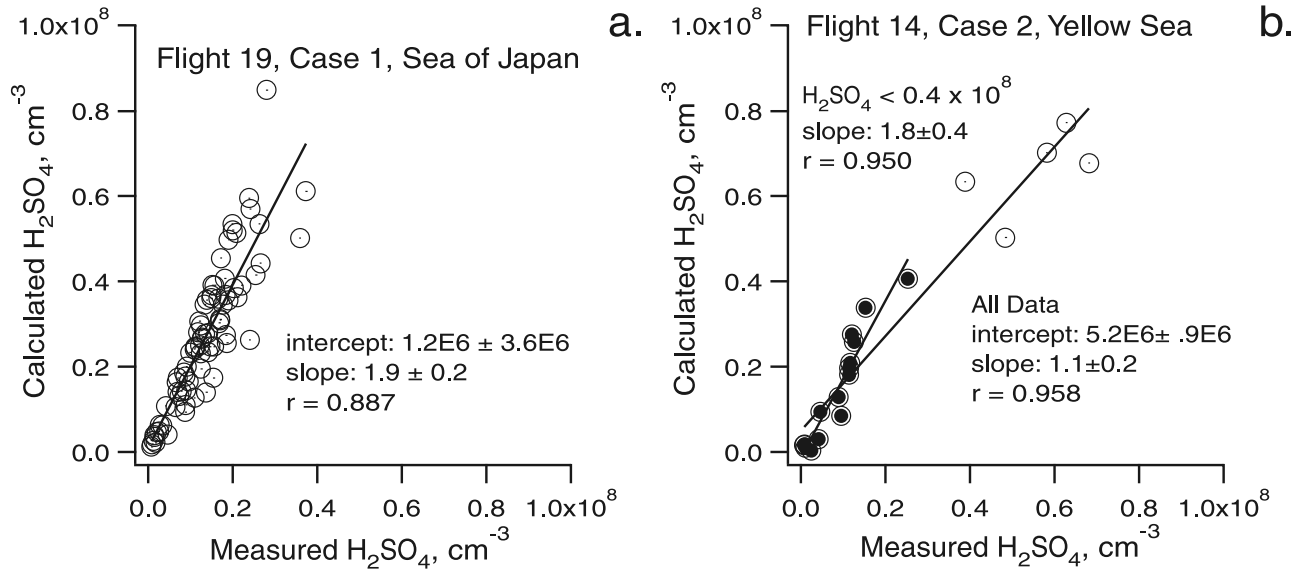

Figure 10. Comparison between measured and calculated H_2SO_4 concentrations assuming steady state balance between OH-SO_2 production and loss onto preexisting particles. The data is for the regions near and within the plumes shown in Figures 3 and 7. In Figure 10b, the regression for H_2SO_4 concentrations less than 4×10^7 cm^{-3} is also shown with the regression for all data plotted.

more dominant factor; OH concentrations in the Yellow Sea plume are a factor of 2 larger and SO_2 a factor of 4 larger.

[39] The interaction between H_2SO_4 production and loss by scavenging can be used to predict ambient H_2SO_4 concentrations. The consistency between the measurements of SO_2, H_2SO_4, and the preexisting aerosol is investigated by comparing observed and calculated steady state H_2SO_4 concentrations.

5.1. Continuity Between SO_2, H_2SO_4, and the Preexisting Particles

[40] Because SO_2, through the production of H_2SO_4, and the preexisting particles appear to play major roles in determining the production of nanoparticles near and within these plumes, the continuity between these measurements is investigated. Ambient H_2SO_4 concentrations are calculated by equation (3), which assumes a steady state between the acid source via OH-SO_2 reaction, equation (2), and sink by preexisting particle scavenging. This is likely a good assumption since the acid production and loss rates in these plumes are high (e.g., 10^5 to 10^6 cm^{-3} s^{-1}), and thus the concentrations respond rapidly to changes in production and scavenging rates. A similar analysis for measurements in clean remote regions show that calculated and measured concentrations of H_2SO_4 are typically in good agreement [*Eisele and Tanner*, 1993; *Weber et al.*, 1997].

[41] The results of this calculation for the measurements near and within the plumes shown in Figures 3 and 7 are summarized in Figure 10. For the Sea of Japan plume of Flight 19, case 1, the calculated H_2SO_4 is approximately twice the observed. Measured and calculated H_2SO_4 concentrations are in fairly close agreement for the more polluted Yellow Sea plume of Flight 14, case 2, where the slope is within 10%. However, when only observer H_2SO_4 concentrations less than 4×10^7 cm^{-3} are included (concentrations similar to Flight 19), the calculated concentrations are also over predicted by a factor of ~2. Thus it is only under the highest acid concentration in the Yellow Sea that the measured and predicted H_2SO_4 are similar. At other times, the predicted concentrations are too high. In both cases the correlation is fairly high indicating that the trends in the measured H_2SO_4 are captured by the variations in SO_2, OH, and aerosol distribution.

[42] The cause for the over-predicted concentration is not known. It could be that the measure SO_2 or OH concentrations are too high, the measured H_2SO_4 is too low, or that the measured preexisting particle distribution is too low. (The uncertainty in accommodation coefficient seems an unlikely cause since a value near one was assumed). The aerosol distribution used to calculate the Fuch and Sutugin mass transfer rates is the most uncertain. The mass transfer rates may be too low for a number of reasons: First, the complete distribution is not measured. However, Figure 11 shows surface area distributions for measurements within the two plumes. The plot shows that most of the H_2SO_4 uptake is in the accumulation mode by particles between 0.1 and 1 μm diameter and that most of the distribution is apparently measured by the optical particle counter. Fuchs-Sutugin mass uptake rate constants in which particles smaller than 0.1 μm are included (measured with a differential mobility analyzer) and increased by less than 10%, so the role of smaller particles is minor and can be ignored. A second uncertainty associated with the preexisting particle distribution is that the calculation of the ambient wet distribution from measured dry distributions underestimates the amount of water uptake by the particles. However, the bulk particle ionic composition for particles less than roughly 1.3 μm diameter, shown in Figures 5 and 9, are very similar for the two plumes, even in the regions of highest acid concentrations in Flight 14, case study 2 where measured and predicted H_2SO_4 concentrations tended to agree. In all cases, the ionic components of the aerosol particles are ammonium nitrate and sulfate salts. In the current analysis, the coarse particles are not assumed to take

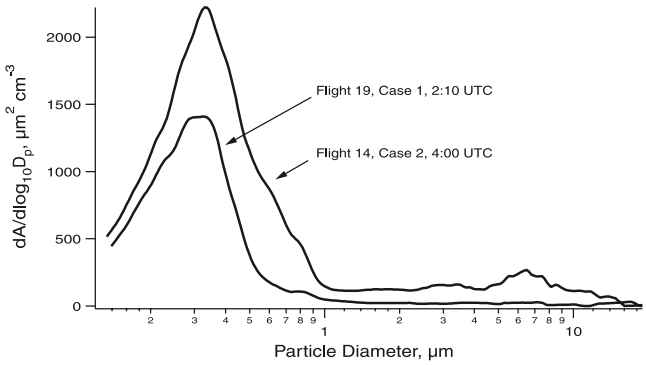

Figure 11. Surface area size distributions calculated from number distributions measured with an optical particle counter with inlet heated to 40°C. Particles are grown to ambient RH assuming uptake is by dust particles.

up water. Repeating the calculations assuming coarse sea-salt particles does not significantly change the predicted H_2SO_4 concentrations. Thus although we lack an explanation for the discrepancy, the trends in the SO_2, H_2SO_4, and preexisting particles are consistent.

[43] Finally, this analysis shows that H_2SO_4 and preexisting aerosol particle concentrations are coupled through scavenging. As the plume ages, H_2SO_4 concentrations should drop. At some point, new particle formation should cease due to the combined effect of reduction in SO_2 as it is consumed (reducing H_2SO_4 production rates), and an increase in the rate of H_2SO_4 scavenged as gas-to-particle conversion over time increases the aerosol surface area. Clearly, the plumes we have investigated have not reached that point. An idea on how long it takes for a typical plume to reach that point would be of interest from both a health effects and a radiative forcing standpoint. Model predictions could provide insight into the timescales for quenching nucleation in these types of plumes.

5.2. Nucleation Mechanism

[44] The plumes discussed in this paper contain the highest 3 to 4-nm particle concentrations recorded during TRACE-P. The mechanism that led to particle production remains unclear. However, the observations are not well explained by some theories. The data suggests H_2SO_4 plays a role, and most nucleation mechanisms assume the same. Predictions for binary H_2SO_4-H_2O nucleation rates using current models [*Kulmala et al.*, 1998] suggest that H_2SO_4 concentrations of roughly two orders of magnitude higher than those observed are necessary for particle production in these regions.

[45] The inability of binary nucleation to predict the observations in the anthropogenic plumes is further demonstrated by comparing the anthropogenic plumes to the volcanic plume intercepted on flight 17, emanating from Miyake-Jima, on the Island of Izu, Japan (34.08°N, 139.53°E). This plume is identified by high SO_2 (often over 10 ppbv) and very low CO concentrations (217 ppbv). The 5-day back trajectories also confirm emissions from Miyake-Jima. Data from this plume are summarized in Table 2e.

[46] A comparison between the concentrations of newly formed 3 to 4-nm particles and H_2SO_4 concentrations in the nucleation regions of the two pollution plume case studies and those in the volcanic plume is shown in Figure 12. In the anthropogenic plumes, higher nanoparticle concentrations are associated with higher H_2SO_4 concentrations but not for the volcanic plume. Binary nucleation rates depend mainly on the relative humidity and H_2SO_4 relative acidity. Comparisons based on data from Table 2 show that the conditions most optimal for binary nucleation are found in the volcanic plume. Both the relative humidity and acidity is higher than in the 3 to 4-nm regions of flight 14 and 19 plumes. The measurement of few 3 to 4-nm particles in the volcanic plume compared to the anthropogenic plumes is further evidence that other gaseous species are required for particle production and that binary H_2SO_4-H_2O nucleation can likely be excluded as the mechanism.

[47] Modeling [*Kerminen et al.*, 2001; *Korhonen et al.*, 1999] and experimental results [*Ball et al.*, 1999] show nucleation is possible at H_2SO_4 concentrations on the order of 10^7 cm^{-3} if NH_3 is greater than 20 pptv (25°C). These acid concentrations are similar to our observations. Although NH_3 was not measured, the fine particle ionic composition data suggest significant levels of NH_3 were likely associated with the plumes, based on particulate ammonium (NH_4^+) as an indirect indicator for the availability of NH_3. Figures 5 and 9 show that NH_4^+ was the main neutralizing agent of the acid aerosol species, with concentrations much higher than the other aerosol cations (i.e., Na^+, K^+, Mg^{2+}, and Ca^{2+}), and a significant amount of the ammonium was likely in the form of ammonium nitrate (NH_4NO_3). Since NH_4NO_3 will only form once all sulfate aerosol is neutralized [*Seinfeld and Pandis*, 1998], the presence of NH_4NO_3 suggests available NH_3. In the volcanic plume, where no 3 to 4-nm particles were observed, there was insufficient NH_4^+ to neutralize the SO_4^{2-}. NH_4^+/SO_4^{2-} molar ratios in the volcanic plumes were typically less than 1. Thus the fine particle data supports the view that the anthropogenic plumes were not depleted of NH_3 and the volcanic plume was depleted. Note that nucleation mechanisms other than H_2SO_4-NH_3-H_2O are possible. However, the data suggests that particle production in these plumes

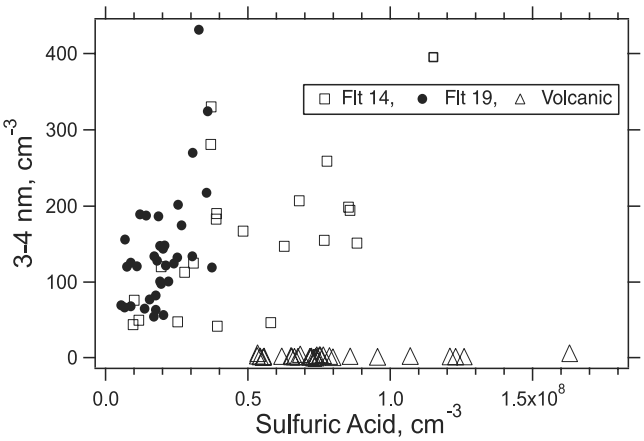

Figure 12. Comparison of the sulfuric acid concentrations and 3 to 4-nm particles concentrations in the nucleation regions of the two plumes investigated and in a volcanic plume. The data suggests that gaseous precursors other than H_2SO_4 are also required for particle formation.

was limited by H_2SO_4 concentrations and that other species associated with the plumes also played a role.

6. Summary

[48] Measurements near the sources of Asian outflow from populated regions provided an opportunity to study new particle formation in anthropogenic plumes. Based on simultaneous measurements of various parameters, H_2SO_4 and the aerosol surface area concentrations appear to have the largest influence on 3 to 4-nm particle concentrations. The characteristic lifetime of these particles due to scavenging by the larger particles is estimated to be less than approximately 15 min. Thus the particles were likely to have been recently produced in situ by homogeneous nucleation.

[49] Two different anthropogenic plumes are investigated in detail. In both, distinct increases in 3 to 4-nm particle concentrations are found in regions of high H_2SO_4 and surface areas that are low or decreasing relative to immediate surroundings and often correspond to dryer regions. These regions were observed near the edges of the plumes where dilution had occurred and in one case within the plume itself. For a plume observed in the Sea of Japan, nucleation was only observed in the near-plume field where dilution appears to play a key role in producing conditions for nucleation. For this plume, SO_2 concentration of $\sim$2 ppbv, and surface areas of $\sim$20 $\mu m^2 cm^{-3}$ resulted in H_2SO_4 concentrations of $\sim 2 \times 10^7$ cm^{-3} (2°C), and nucleation. No 3 to 4-nm particle production was observed within this plume despite similar H_2SO_4 concentrations, however, particle surface areas were much higher at 170 μm^2 cm^{-3}. In contrast, nucleation was observed above, within the dilution region, and within the most heavily polluted plume encountered on the NASA P3 aircraft during TRACE-P. In this case, particle production was observed in a region where SO_2 concentrations were roughly 8 ppbv, particle surface areas of $\sim$750 $\mu m^2 cm^{-3}$, and H_2SO_4 concentrations of 1 to 6 $\times$ 10^7 cm^{-3} (10°C). Nearby, within the center of the plume, no nucleation was observed where SO_2 levels were 3 pptv and surface areas were 1600 $\mu m^2 cm^{-3}$. These results show that even highly polluted plumes with high aerosol surface area concentrations can support regions of new particle formation if SO_2 concentrations are sufficient.

[50] Contrasting these plumes to a volcanic plume of higher H_2SO_4 concentrations but with few 3 to 4-nm particles shows that nucleation was not via a binary H_2SO_4 and H_2O mechanism. Measurements of the fine particle ionic composition indicates that both plumes have ammonium to sulfate molar ratios from three to five in the nucleation regions due to the presence of ammonium nitrate, compared with molar ratios less than 1 in the volcanic plume. These results are consistent with the presence of excess ammonia in the nucleating plumes; this suggests the possible participation of ammonia through a ternary H_2SO_4-NH_3-H_2O mechanism.

[51] **Acknowledgments.** The authors gratefully acknowledge the support of the National Atmospheric and Space Administration (NASA) under grant number NCC-1-411L. We also thank the many people from NASA Langley and the NASA Wallops Flight Facility for all their help during the experiment.

References

Ayers, G. P., R. W. Gillett, and J. L. Gras, On the vapor pressure of sulfuric acid, *Geophys. Res. Lett.*, *7*, 7433–7436, 1980.

Ball, S. M., D. R. Hanson, F. L. Eisele, and P. H. McMurry, Laboratory studies of particle nucleation: Initial results for H_2SO_4, H_2O, and NH_3 vapors, *J. Geophys. Res.*, *104*, 23,709–23,718, 1999.

Birmili, W., and A. Wiedensohler, New particle formation in the continental boundary layer: Meteorological and gas phase parameter influence, *Geophys. Res. Lett.*, *27*, 3325–3328, 2000.

Birmili, W., A. Wiedensohler, C. Plass-Dulmer, and H. Berresheim, Evolution of newly formed aerosol particles in the continental boundary layer: A case study including OH and H_2SO_4 measurements, *Geophys. Res. Lett.*, *27*, 2205–2208, 2000.

Brock, C. A., et al., Particle growth in the plumes of coal-fired power plant, *J. Geophys. Res.*, *108*(D3), 4111, doi:10.1029/2002JD002746, 2003.

Coffman, D. J., and D. A. Hegg, A preliminary study of the effect of ammonia on particle nucleation in the marine boundary layer, *J. Geophys. Res.*, *100*, 7147–7160, 1995.

DeMore, W. B., S. P. Sander, D. M. Golden, R. F. Hampson, M. J. Kurylo, C. J. Howard, A. R. Ravishankara, C. E. Kolb, and M. J. Molina, Chemical kinetics and photochemical data for use in stratospheric modeling, *Eval. 10*, pp. 20–92, Jet Propul. Lab., Pasadena, Calif., 1992.

Donaldson, K., X. Y. Li, and W. MacNee, Ultrafine (nanometer) particle mediated lung injury, *J. Aerosol Sci.*, *29*, 553–560, 1998.

Eisele, F. L., and D. J. Tanner, Measurements of the gas phase concentrations of H_2SO_4 and methane sulfonic acid and estimates of H_2SO_4 production and loss in the atmosphere, *J. Geophys. Res.*, *98*, 9001–9010, 1993.

Eisele, F. L., G. H. Mount, F. C. Fehsenfeld, J. Harder, E. Marovich, J. Roberts, D. J. Tanner, and M. Trainer, An intercomparison of tropospheric OH and ancillary trace gas measurements at Fritz Peak Observatory, Colorado, *J. Geophys. Res.*, *99*, 18,605, 1994.

Eisele, F. L., R. L. Mauldin III, D. J. Tanner, J. R. Fox, T. Mouch, and T. Scully, An inlet sampling duct for airborne OH and sulfuric acid measurements, *J. Geophys. Res.*, *102*, 27,993–28,002, 1997.

Ferin, J., Oberdorster, D. P. Penney, S. C. Soderholm, R. Gelein, and H. C. Piper, Increased pulmonary toxicity of ultrafine particles? I. Particle clearance, translocation, morphology, *J. Aerosol Sci.*, *21*, 381–384, 1990.

Fuchs, N. A., and A. G. Sutugin, *Highly Dispersed Aerosols*, pp. 47–60, Butterworth-Heinemann, Woburn, Mass., 1970.

Fuelberg, H. E., J. R. Hannan, P. F. J. Van Velthoven, E. V. Browell, G. Bieberbach Jr., R. D. Knabb, G. L. Gregory, K. E. Pichering, and H. B. Selkirk, A meteorological overview of the SONEX period, *J. Geophys. Res.*, *105*, 3633–3651, 2000.

Gmitro, J., and T. Vermeulen, Vapor-liquid equilibrium for aqueous sulfuric acid, *UCRL-10886, LRL Rep., TID-4500*, Univ. of Calif., Berkeley, Berkeley, Calif., 1963.

Jacob, D. J., J. H. Crawford, M. M. Kleb, V. E. Connors, R. J. Bendura, J. L. Raper, G. W. Sachse, J. C. Gille, and L. Emmons, Transport and Chemical Evolution over the Pacific (TRACE-P) mission: Design, execution, and first results, *J. Geophys. Res.*, *108*(D20), 9000, doi:10.1029/2002JD003276, in press, 2003.

Jefferson, A., F. L. Eisele, P. J. Ziemann, J. J. Marti, R. J. Weber, and P. H. McMurry, Measurements of the H_2SO_4 mass accommodation coefficient onto polydisperse aerosol, *J. Geophys. Res.*, *102*, 19,021–19,028, 1997.

Jefferson, A., D. J. Tanner, F. L. Eisele, and H. Berresheim, Sources and sinks of H_2SO_4 in the remote Antarctic marine boundary layer, *J. Geophys. Res.*, *103*, 1639–1645, 1998.

Kerminen, V. M., L. Pirjola, and M. Kulmala, How significantly does coagulational scavenging limit atmospheric particle production?, *J. Geophys. Res.*, *106*, 24,119–24,125, 2001.

Korhonen, K., M. Kulmala, A. Laaksonen, Y. Vissanen, R. McGraw, and J. H. Seinfeld, Ternary nucleation of H_2SO_4, NH_3, and H_2O in the atmosphere, *J. Geophys. Res.*, *104*, 26,349–26,353, 1999.

Kulmala, M., A. Laaksonen, and L. Pirjola, Parameterizations for sulfuric acid/water nucleation rates, *J. Geophys. Res.*, *103*, 8301–8307, 1998.

Ma, Y., et al., The characteristics and influence of biomass burning aerosols on fine particle ionic composition measured in Asian Outflows during TRACE-P, *J. Geophys. Res.*, *108*(D2), 8816, doi:10.1029/2002JD003128, in press, 2003.

Maloney, J. C., H. E. Fuelberg, M. A. Avery, J. H. Crawford, D. R. Blake, B. G. Heikes, G. W. Sachse, G. T. Sandholm, H. Singh, and R. W. Talbot, Chemical characteristics of air from different source regions during the second Pacific Exploratory Mission in the Tropics, *J. Geophys. Res.*, *106*, 32,609–32,625, 2001.

Marti, J. J., R. J. Weber, M. T. Saros, J. G. Vasiliou, and P. H. McMurry, Technical note: Modification of the TSI 3025 condensation particle counter for pulse height analysis, *Aerosol Sci. Technol.*, *25*, 214–218, 1996.

McMurry, P. H., K. S. Woo, R. J. Weber, D.-R. Chen, and D. Y. H. Pui, Size distributions of 3–10 nm atmospheric particles: Implication for nuclea-

tion mechanisms, *Phil. Trans. R. Soc. London, Ser. A*, *358*, 2625–2642, 2000.

Orsini, D., Y. Ma, A. Sullivan, B. Sierau, K. Baumann, and R. J. Weber, Refinements to the particle-into-liquid sampler (Pils) for ground and airborne measurements of water soluble aerosol composition, *Atmos. Environ.*, *37*, 1243–1259, 2003.

Roedel, W., Measurement of sulfuric acid saturation vapor pressure; Implications for aerosol formation by heteromolecular nucleation, *J. Aerosol Sci.*, *10*, 375–386, 1979.

Seinfeld, J. H., and S. N. Pandis, *Atmospheric Chemistry and Physics: From Air Pollution to Climate Change*, John Wiley, Hoboken, N. J., 1998.

Swietlicki, E., et al., Hygroscopic properties of aerosol particles in the north-eastern Atlantic during ACE-2, *Tellus, Ser. B*, *52*, 201–227, 2000.

Tang, Y., et al., Impacts of aerosols and clouds on photolysis frequencies and photochemistry during TRACE-P: 2. Three-dimensional study using a regional chemical transport model, *J. Geophys. Res.*, *108*(D21), 8822, doi:10.1029/2002JD003100, in press, 2003.

Thornton, D. C., A. R. Bandy, F. H. Tu, B. W. Blomquist, G. M. Mitchell, W. Nadler, and D. H. Lenschow, Fast airborne sulfur dioxide measurements by atmospheric pressure ionization mass spectrometry (APIMS), *J. Geophys. Res.*, *107*(D22), 4632, doi:10.1029/2002JD002289, 2002.

Weber, R. J., J. J. Marti, P. H. McMurry, F. L. Eisele, D. J. Tanner, and A. Jefferson, Measurements of expected nucleation precursor species and 3 to 500 nm diameter particles at Mauna Loa Observatory, Hawaii, *J. Geophys. Res.*, *101*, 14,767–14,775, 1995.

Weber, R. J., J. J. Marti, P. H. McMurry, F. L. Eisele, D. J. Tanner, and A. Jefferson, Measured atmospheric new particle formation rates: Implications for nucleation mechanisms, *Chem. Eng. Commun.*, *151*, 53–64, 1996.

Weber, R. J., J. J. Marti, P. H. McMurry, F. L. Eisele, D. J. Tanner, and A. Jefferson, Measurements of new particle formation and ultrafine particle growth rates at a clean continental site, *J. Geophys. Res.*, *102*, 4375–4385, 1997.

Weber, R. J., P. H. McMurry, L. Mauldin, D. J. Tanner, F. L. Eisele, F. J. Brechtel, S. M. Kreidenweis, G. L. Kok, R. D. Schillawski, and D. Baumgardner, A study of new particle formation and growth involving biogenic and trace gas species measured during ACE 1, *J. Geophys. Res.*, *103*, 16,385–16,396, 1998a.

Weber, R. J., M. Stolsenburg, S. Pandis, and P. H. McMurry, Inversion of UCNC pulse height distributions to obtain ultrafine (~3 to 10 nm) particle size distributions, *J. Aerosol. Sci.*, *29*, 601–615, 1998b.

Weber, R. J., A. D. Clarke, M. Litchy, J. Li, G. Kok, R. D. Schillawski, and P. H. McMurry, Spurious aerosol measurements when sampling from aircraft in the vicinity of clouds, *J. Geophys. Res.*, *103*, 28,337–28,346, 1998c.

Weber, R. J., P. H. McMurry, R. L. Mauldin III, D. J. Tanner, F. L. Eisele, A. D. Clarke, and V. N. Kapustin, New particle formation in the remote troposphere: A comparison of observations at various sites, *Geophys. Res. Lett.*, *26*, 307–310, 1999.

Weber, R. J., G. Chen, D. D. Davis, R. L. Mauldin, D. J. Tanner, F. L. Eisele, A. D. Clarke, D. C. Thornton, and A. R. Bandy, Measurements of enhanced H_2SO_4 and 3–4 nm particles near a frontal cloud during ACE 1, *J. Geophys. Res.*, *106*, 24,107–24,117, 2001a.

Weber, R. J., D. Orsini, Y. Daun, Y. N. Lee, P. J. Klotz, and F. Brechtel, A particle-into-liquid collector for rapid measurements of aerosol bulk chemical composition, *Aerosol Sci. Technol.*, *35*, 718–727, 2001b.

Wilemski, G., Composition of the critical nucleus in multicomponent vapor nucleation, *J. Chem. Phys.*, *80*, 1370–1372, 1984.

Williams, D. J., J. N. Carras, J. W. Milne, and A. C. Heggie, The oxidation and long-range transport of sulphur dioxide in a remote region, *Atmos. Environ.*, *15*, 2255–2262, 1981.

Wilson, W. E., Sulfates in the atmosphere: A progress report on project MISTT, *Atmos. Environ.*, *12*, 537–547, 1978.

Woo, K. S., D. R. Chen, D. Y. H. Pui, and P. H. McMurry, Measurement of Atlanta aerosol size distributions: Observations of ultrafine particle events, *Aerosol Sci. Technol.*, *34*, 75–87, 2001.

Yu, F., and R. P. Turco, From molecular clusters to nanoparticles: Role of ambient ionization in troposperic aerosol formation, *J. Geophys. Res.*, *106*, 4797–4814, 2001.

A. R. Bandy and D. C. Thornton, Department of Chemistry, Drexel University, Philadelphia, PA 19104, USA. (bandyar@drexel.edu; dct@drexel.edu)

C. Cantrell, F. Eisele, E. Kosciuch, and L. Mauldin, National Center for Atmospheric Research, 1850 Table Mesa, Boulder, CO 80303, USA. (cantrell@ucar.edu; eisele@ucar.edu; kosciuch@ucar.edu; mauldin@ucar.edu)

A. D. Clarke, V. Kapustin, and K. Moore, Department of Oceanography, University of Hawaii at Manoa, 1000 Pope Road, Honolulu, HI 96822, USA. (tclarke@soest.hawaii.edu; kapustin@soest.hawaii.edu; kmoore@soest.hawaii.edu)

G. Chen and G. W. Sachse, NASA Langley Research Center, Mail Stop 401B, Hampton, VA 23681, USA. (g.chen@express.larc.nasa.gov; g.w.sachse@larc.nasa.gov)

H. E. Fuelberg, Department of Meteorology, Florida State University, Tallahassee, FL 32306, USA. (fuelberg@huey.met.fsu.edu)

S. Lee and R. J. Weber, School of Earth and Atmospheric Sciences, Georgia Institute of Technology, 311 Ferst Dr., Atlanta, GA 30332-0340, USA. (rweber@eas.gatech.edu; gte822w@prism.gatech.edu)

B. Wang, QuadraMed Corporation, 12110 Sunset Hills Road, #600, Reston, VA 20190, USA. (pwang@quadramed.com)